Vibronic collapse of ordered quadrupolar ice in the pyrochlore magnet $Tb_{2+x}Ti_{2-x}O_{7+y}$

Y. Alexanian,[1,*] J. Robert,[1] V. Simonet,[1] B. Langérôme,[2] J.-B. Brubach,[2] P. Roy,[2] C. Decorse,[3] E. Lhotel,[1] E. Constable,[4,1] R. Ballou,[1] and S. De Brion[1,†]

[1]*Université Grenoble Alpes, CNRS, Institut Néel, 38000 Grenoble, France*
[2]*Synchrotron SOLEIL, L'Orme des Merisiers, 91192 Gif-sur-Yvette, France*
[3]*ICMMO, Université Paris-Saclay, CNRS, 91400 Orsay, France*
[4]*Institute of Solid State Physics, TU Wien, 1040 Vienna, Austria*

(Received 20 July 2022; revised 17 May 2023; accepted 19 May 2023; published 8 June 2023)

While the spin-liquid state in the frustrated pyrochlore $Tb_{2+x}Ti_{2-x}O_{7+y}$ has been studied both experimentally and theoretically for more than two decades, a definite description of this unconventional state still needs to be achieved. Using synchrotron-based THz spectroscopy in combination with quantum numerical simulations, we highlight a significant link between two features: the existence of a quadrupolar order following an ice rule and the presence of strong magnetoelastic coupling in the form of hybridized Tb^{3+} crystal-field and phonon modes. The magnitude of this so-called vibronic process, which involves quadrupolar degrees of freedom, is significantly dependent on small off-stoichiometry x and favors all-in–all-out-like correlations between quadrupoles. This mechanism competes with the long-range ordered quadrupolar ice, and for slightly different stoichiometry, is able to destabilize it.

DOI: 10.1103/PhysRevB.107.224404

I. INTRODUCTION

Quantum materials have attracted considerable interest lately. A wide spectrum of exotic behaviors built upon magnetic dipolar degrees of freedom were already discovered and are still foreseen. Among them, one finds those induced through magnetic frustration such as quantum spin liquids with fractional or anyonic excitations to quote but one example [1,2]. Another emblematic geometric frustration-induced state is the classical spin ice, as observed in $Ho_2Ti_2O_7$ [3], belonging to the pyrochlore family $R_2M_2O_7$, where the magnetic rare-earth ions R^{3+} form a corner-sharing tetrahedra network [4]. Spin ice correlations are characterized by the ice rule (two spins pointing into and two out of each tetrahedron), which can be destabilized towards an exotic ordered/disordered fragmented state when additional competing all-in–all-out correlations (all spins pointing into or out of each tetrahedron) are present [5–7]. A novel field of unconventional behaviors induced by frustration has recently emerged, involving multipolar degrees of freedom that come into play once the angular momenta are larger than one half. A case in point is provided by the rare-earth-based compounds [8], the description of which sometimes requires Hamiltonians involving quadrupoles [9–11] or even multipoles of higher orders, such as recently shown in Ce-, Pr-, or Nd-based pyrochlores [12–19]. These multipoles are governed by the nature of the magnetic ion as well as their local environment, the so-called crystal field that lifts the degeneracy of their electronic levels. Extensions of theses degrees of freedom to composite hidden order [20] were also considered that might be relevant to quite different quantum materials such as high-temperature superconductors [21,22]. Here, we focus on quadrupolar degrees of freedom and show how they play a crucial role in the exotic and still enigmatic behavior of the pyrochlore compound $Tb_2Ti_2O_7$. First studies on $Tb_2Ti_2O_7$ more than two decades ago showed that no long-range magnetic order is stabilized down to at least 70 mK [25,26]. The compound remains in an intriguing spin-liquid state quite different from conventional spin ices, although similarities have been observed [27,28]. While it was quickly noticed that the presence of a Tb^{3+} excited crystal-field level as low as $\Delta = 1.5$ meV (12 cm^{-1}) [26,29–36] certainly has a central role in this exotic quantum state [37,38], any tentative description of the fundamental state failed to reproduce all experimental data [28,39–44]. In the past decade, two important steps were achieved almost simultaneously. On one hand, it was realized (based on specific heat [23,24] and latter supported by elastic constants [45] measurements), that $Tb_{2+x}Ti_{2-x}O_{7+y}$ has a strong sensitivity to a very low antisite Tb/Ti disorder. For the off-stoichiometry parameter $x \gtrsim 0$, it enters into a quadrupolar long-range ordered phase below $T_c \approx 0.5$ K [46–51]. On the other hand, while no static distortion is observed [31,52–56], extensive neutron scattering [57–61] and THz spectroscopy measurements [62,63] have revealed the presence of several magnetoelastic modes. In particular, it was shown that a so-called vibronic process [64] develops below 50 K and mixes the ground and first excited Tb^{3+} crystal-field doublets with acoustic phonons [62]. A second vibron, visible below 200 K, couples the first excited doublet with a silent optical phonon mode [62].

In this paper, we used synchrotron-based THz spectroscopy to provide evidence for a competition between

*Present address: Department of Quantum Matter Physics, University of Geneva, 24 Quai Ernest-Ansermet, 1211 Geneva, Switzerland; yann.alexanian@unige.ch
†sophie.debrion@neel.cnrs.fr

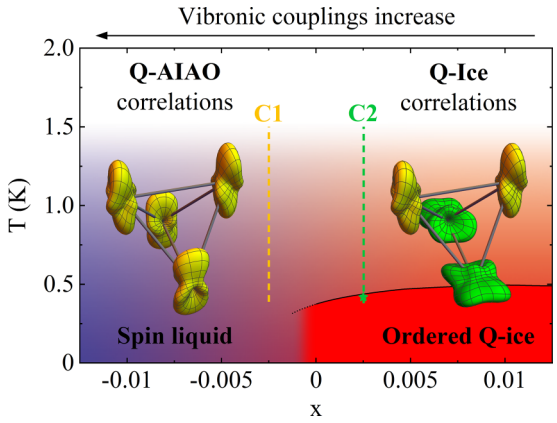

FIG. 1. $Tb_{2+x}Ti_{2-x}O_{7+y}$ phase diagram as a function of the temperature and the off-stoichiometry x deduced from this work and from Refs. [23,24]. Quadrupolar all-in–all-out-like correlations are favored by vibronic couplings for $x \lesssim 0$ while quadrupolar ice correlations are promoted by multipolar interactions for $x \gtrsim 0$ leading to an ordered quadrupolar ice at low temperatures. Our two single crystals C1 and C2 have been characterized by specific heat measurements in the temperature range shown by the dashed lines. C2 orders below 0.42 K (green star). The configuration of the four quadrupoles on one tetrahedron in both regions is displayed.

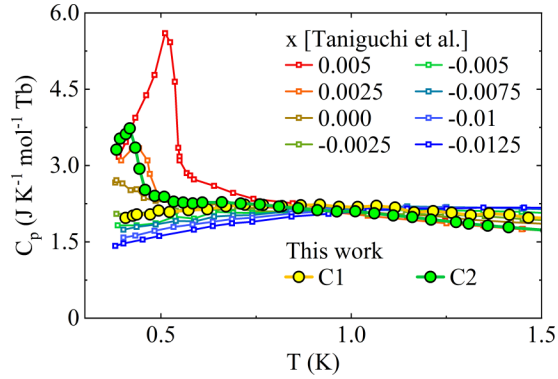

FIG. 2. $Tb_{2+x}Ti_{2-x}O_{7+y}$ specific heat as a function of temperature for different off-stoichiometry x. Solid symbols: this study for crystals C1 (yellow) and C2 (green). Open symbols: data from Ref. [23]. The comparison of both data sets allows us to deduce that $x \approx -0.0025$ for C1 and $x \approx +0.0025$ for C2.

the previously described vibronic processes and the low-temperature quadrupolar order of $Tb_{2+x}Ti_{2-x}O_{7+y}$ (see Fig. 1). Our measurements reveal that the spin lattice couplings are stronger when $x < 0$ than $x > 0$. We then show that these couplings promote quadrupolar all-in–all-out-like correlations (Q-AIAO), which compete with the quadrupolar ice-like correlations (Q-Ice) that prevails for $x \gtrsim 0$, where an ordered quadrupolar ice is finally stabilized at very low temperature. The spin-liquid state of $Tb_{2+x}Ti_{2-x}O_{7+y}$ compounds with $x \lesssim 0$ is therefore caused by a subtle equilibrium between magnetic interactions and the competition between these two types of quadrupolar correlations.

II. EXPERIMENTAL RESULTS AND DISCUSSION

A. THz measurements

High-resolution THz spectroscopy measurements were performed at Synchrotron SOLEIL on the AILES beamline from 200 to 6 K in the 8–24 cm^{-1} range (resolution 0.2 cm^{-1}) on a C2 crystal, previously used in a magneto-optical study [63]. We measured two different plaquettes cut out of this crystal, perpendicular to a $\langle 111 \rangle$ and $\langle 110 \rangle$ direction of the cubic pyrochlore lattice (thickness 150 μm/170 μm, diameter 1.7 mm/1.2 mm, respectively). The experimental conditions were the same as the high-resolution THz study previously done on another crystal C1 [62], whose results are shown in the present paper to allow a direct comparison between the two crystals. To determine their position in the phase diagram as a function of the off-stoichiometry, they were both characterized by specific heat measurements in the temperature range 10–400 K owing to a physical property measurement system (PPMS) with a ^{3}He insert, using the same samples. THz absorption spectra were calculated solving Maxwell equations with the magnetic susceptibility tensor deduced from eigenenergies and eigenvectors of the Hamiltonian [63,65]. Absorption peaks were modeled by the same pseudo-Voigt function $0.7L + 0.3G$, where L and G are Lorentzian and Gaussian functions with the same width at half maximum chosen equal to 2.7 cm^{-1}, in agreement with the observed linewidth of Ref. [62] on the C1 sample. The specific heat characterization for the two crystals is given in Fig. 2 and, to evaluate their off-stoichiometry, compared to measurements on samples with different x values from Ref. [23]. A clear peak is visible for C2 at $T_c = 0.42$ K, which yields $x \approx +0.0025$. This peak reveals the onset of a quadrupolar order. Quite differently, no peak is observed in C1, confirming that this crystal, whose off-stoichiometry is estimated to $x \approx -0.0025$, presents a quadrupolar order but remains in a spin-liquid state [28].

The THz spectroscopy results on crystal C2 are presented in Fig. 3 for different temperatures, together with those previously obtained on crystal C1. In Figs. 3(a) and 3(b), the reference spectrum is taken at 200 K. The broad absorption peak, centered around 14 cm^{-1}, is observed in both samples and is assigned to the first Tb^{3+} crystal-field excited doublet. Another smaller peak centered around 22 cm^{-1} is present in the C1 spectra only, called P3 in Ref. [62], is experimental evidence of the high-temperature vibronic process: While coupling with the first crystal-field excited level, the transverse optical phonon, initially infrared inactive, becomes visible. Results on C2 reveal that P3 is absent, showing that this magnetoelastic process seems not to take place.

To highlight the off-stoichiometry impact on the low-temperature vibronic process, Figs. 3(c) and 3(d) show the same spectra but with a 60 K reference, a significantly lower temperature where the high-temperature vibronic process observed in C1 becomes temperature independent. The previous results for crystal C1 that are reproduced here show a fine structure: Besides the central peak P1 at 13.8 cm^{-1}, another one, P2, is observed at 16.8 cm^{-1}. Further analysis [62] shows that a third peak, P0, is also present at 11 cm^{-1}. These three peaks were associated to a splitting of the ground and first crystal-field excited doublets due to the low-temperature vibronic process that involves acoustic phonons. Quite surprisingly, for C2, we only observe one single peak. Note also that spectra with different wave polarizations or wave vectors

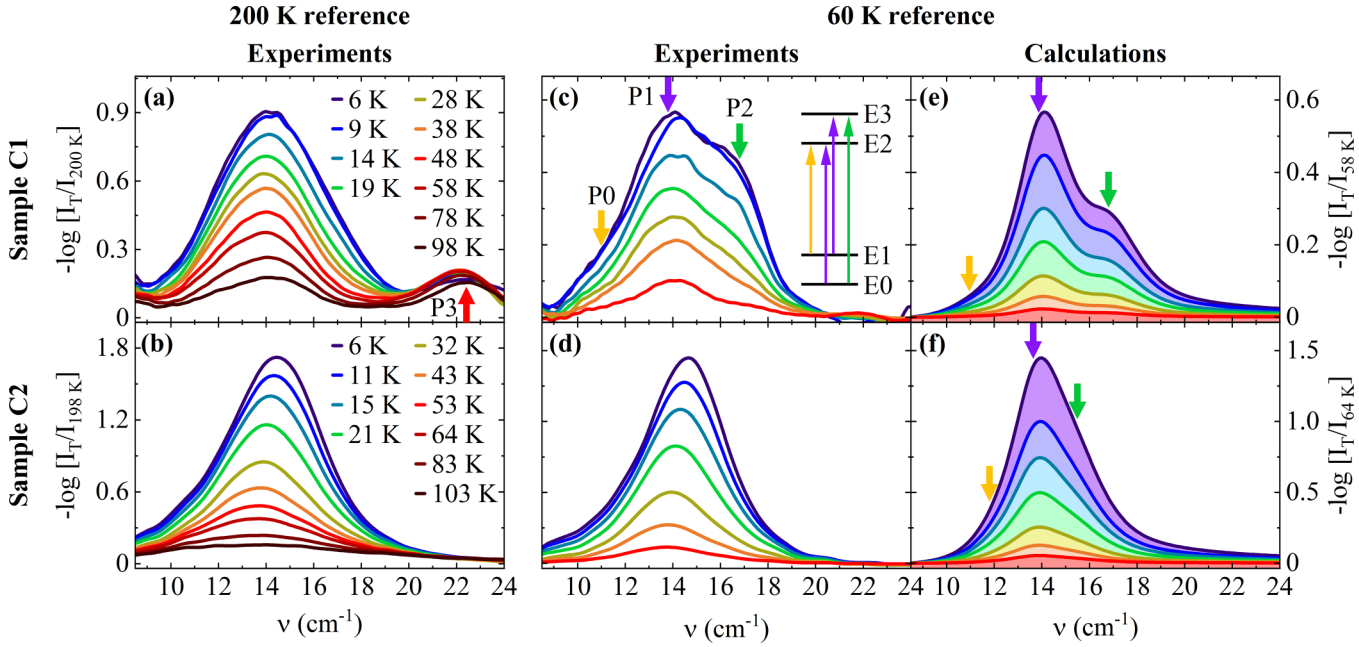

FIG. 3. $Tb_{2+x}Ti_{2-x}O_{7+y}$ THz spectra as a function of temperature for crystal C1 (upper panels) and C2 (lower panels). These differential absorptions are calculated by dividing the sample spectrum of interest by one at a higher temperature chosen to emphasize different processes: (a), (b) with a high-temperature reference $T \approx 200$ K, and (c), (d) with a low-temperature reference $T \approx 60$ K. Calculations of the same quantity with the low-temperature reference for a vibronic parameter (e) $D = -0.38$ meV and (f) $D = -0.24$ meV. The THz wave vector was $\boldsymbol{k} \parallel [111]$ and its polarization $\boldsymbol{e} \parallel [0\bar{1}1]$, $\boldsymbol{h} \parallel [2\bar{1}\bar{1}]$. The measured and calculated positions of the P0–P3 peaks are shown by the arrows. In the inset of (c), the splitting by the vibronic coupling of the two ground and first excited doublets is schematized.

are similar in C2 whereas they vary in C1 (see Supplemental Material [66]). It is intriguing that the fine structure of C1 is not visible in C2, all the more so that the influence of the low-temperature vibronic process was observed in the magneto-optical study on this sample: It was a key ingredient to understand the magnetic field dependence of its THz spectra, in particular the splitting of one of the field-induced transition as reported in Ref. [63].

B. THz spectra calculations

To understand these evolutions of the THz spectra, numerical simulations have been carried out using the vibronic model developed previously for crystal C1 [62,63]. Then the Hamiltonian of our simulations contains two parts: the crystal-field Hamiltonian $\widehat{\mathcal{H}}_{\rm cf}$ and the low-temperature vibronic coupling one $\widehat{\mathcal{H}}_{\rm vib}$. Using the local threefold axis of each Tb^{3+} site (point group symmetry $\mathcal{D}_{3d}$) as the quantification z axis, they can be written in the same form for the four Tb^{3+} ions at the vertices of each tetrahedron that constitutes the pyrochlore lattice. In this case, $\widehat{\mathcal{H}}_{\rm cf}$ writes

$$\widehat{\mathcal{H}}_{\rm cf} = \theta_2\lambda_2^0 B_0^2\widehat{\mathcal{O}}_2^0 + \theta_4\big(\lambda_4^0 B_0^4\widehat{\mathcal{O}}_4^0 + \lambda_4^3 B_3^4\widehat{\mathcal{O}}_4^3\big) + \theta_6\big(\lambda_6^0 B_0^6\widehat{\mathcal{O}}_6^0 + \lambda_6^3 B_3^6\widehat{\mathcal{O}}_6^3 + \lambda_6^6 B_6^6\widehat{\mathcal{O}}_6^6\big), \quad (1)$$

where $\widehat{\mathcal{O}}_k^q$ are Stevens operators, B_q^k are crystal-field parameters, θ_k are reduced matrix elements, and λ_k^q are numerical coefficients (see Supplemental Material [66]). For $\widehat{\mathcal{H}}_{\rm vib}$, we used the Hamiltonian first proposed by Thalmeier and Fulde [67] and developed for $Tb_2Ti_2O_7$ in Refs. [62,65], in its simplest form with a single vibronic coupling parameter D, assumed to be the only x-dependent parameter in our calculations:

$$\widehat{\mathcal{H}}_{\rm vib} = \theta_2\lambda_2^1 D\big(\widehat{\mathcal{O}}_2^1 + \widehat{\mathcal{O}}_2^{-1}\big). \quad (2)$$

This effective Hamiltonian is identical to the one describing a static strain. More information can be found in the Supplemental Material [66]. Due to this vibronic process, both the ground and first excited doublets are almost equally split producing three distinct energy levels E_1–E_3 [see inset of Fig. 3(c)] obtained in the calculation by diagonalizing $\widehat{\mathcal{H}}_{\rm cf} + \widehat{\mathcal{H}}_{\rm vib}$ (results given in Table I). For C1, we find good agreement between numerical simulations and experimental results with $D = -0.38$ meV [see Figs. 3(c) and 3(e)]. The calculated peak positions $E_2 - E_1 = 10.9\ \text{cm}^{-1} = \text{P0}$, $E_2 - E_0 = 13.8\ \text{cm}^{-1} \approx \text{P1}$, $E_3 - E_1 = 13.9\ \text{cm}^{-1} \approx \text{P1}$, and $E_3 - E_0 = 16.8\ \text{cm}^{-1} = \text{P2}$ are in remarkable agreement with experimental ones, $\text{P0} = 11.0\ \text{cm}^{-1}$, $\text{P1} = 13.8\ \text{cm}^{-1}$, and $\text{P2} = 16.8\ \text{cm}^{-1}$. Furthermore, our calculations reproduce qualitatively the experimental spectral shape with two clearly visible peaks (P1 and P2) and another one only slightly visible P0. For C2, since no visible signature of the vibronic process is seen, we used the magneto-optical measurements of Ref. [63] (reproduced in the Supplemental Material [66]) to fix the vibronic parameter $D = -0.24$ meV. Using this

TABLE I. Calculated energies of the three first excited levels (in cm^{-1}/meV) of C1 and C2.

	E_1	E_2	E_3
C1 ($D = -0.38$ meV)	2.85/0.35	13.8/1.71	16.8/2.08
C2 ($D = -0.24$ meV)	1.83/0.23	13.6/1.69	15.5/1.92

coupling, the C2 spectrum shape is also well reproduced with one single broad excitation, as observed, embedding the three nonresolved peaks at $E_2 - E_1 = 11.8\ \mathrm{cm}^{-1} = \mathrm{P0}$, $E_2 - E_0 = 13.6\,\mathrm{cm}^{-1} \approx \mathrm{P1}$, $E_3 - E_1 = 13.7\,\mathrm{cm}^{-1} \approx \mathrm{P1}$, and $E_3 - E_0 = 15.5\ \mathrm{cm}^{-1} = \mathrm{P2}$ [see Fig. 3(f)].

We note however that the experimental low-temperature dependence is not well captured in our single parameter model. This might be explained by the influence, below 10 K, of interactions between spins and quadrupole degrees of freedom. Indeed, they are necessary for the onset of quadrupole order below 0.5 K and are also required to understand the observed low-temperature magnetic correlations [49–51]. Nevertheless, our THz observations as well as our vibronic interpretation are rather compatible with published data using optical spectroscopy [31,68] and inelastic neutron scattering [23,49,60]. See details in the Supplemental Material [66]. This being said, our model allows us to understand the differences observed between both samples: The three peaks P0, P1 and P2 are present in both cases and due to vibronic processes but are not experimentally resolved for C2 because of a lower vibronic coupling.

C. Pseudo spin approach for the x dependent phase diagram

To go beyond and study the implication of the x dependence of the vibronic coupling on the ground state of $Tb_{2+x}Ti_{2-x}O_{7+y}$, it is useful to adopt a pseudospin description where the vibronic Hamiltonian acts as a perturbation on the crystal-field ground state doublet. In this approach,

$$\widehat{\mathcal{H}}_{\mathrm{vib}}^{(\mathrm{p.s.})} \propto \theta_2 \lambda_2^1 D(\widehat{\sigma}^x - \widehat{\sigma}^y), \tag{3}$$

where $\widehat{\sigma}^{x,y,z}$ are Pauli matrices (see Supplemental Material [66]). Note that for a non-Kramers ion as Tb^{3+}, the longitudinal (z) pseudospin component of the doublet is related to the magnetic dipolar degree of freedom and can couple to a magnetic field while the transverse (x, y) components represent electric quadrupoles degrees of freedom [12,69,70] that are nonmagnetic. Since the vibronic Hamiltonian has the same form for the four Tb^{3+} ions of a tetrahedron, it will favor an orientation of the transverse components of all the Tb^{3+} ions along the same local direction. This will result in planar ferropseudospin also called Q-AIAO configurations, which may eventually order at low temperature. On the other hand, it has been shown that quadrupolar interactions between Tb^{3+} ions favor a planar antiferropseudospin order [48,51], which corresponds to an ordered ice of transverse pseudospin components [15,71,72]. The corresponding Tb^{3+} electronic densities calculated [73,74] for both Q-AIAO and Q-Ice configurations are represented in Fig. 1 (see Supplemental Material [66]) with distinct colors for the two different quadrupolar states. The picture which emerges in $Tb_{2+x}Ti_{2-x}O_{7+y}$ is thus the following: While Tb-Tb interactions are strong enough to stabilize a long-range ordered quadrupolar ice for $x \gtrsim 0$, they compete with the low-temperature vibronic process which promotes all-in–all-out-like quadrupole correlations. As a consequence, the long-range order is suppressed for $x \lesssim 0$, namely when magnetoelastic couplings are sufficiently strong as observed for crystal C1. For larger negative x values, with possibly even stronger vibronic couplings, we then foresee the existence of an ordered Q-AIAO phase that would be interesting to investigate.

At this stage, it is interesting to point out possible effects of disorder. First, random strains associated to defects caused by the off-stoichiometry have not been considered. An approach similar to the one developed in Ref. [75] would be interesting to develop. The Hamiltonian may have the form of Eq. (2) (see Supplemental Material), the D parameter no longer being uniform. Second, as in other non-Kramer pyrochlores [15,76,77], disorder may produce competition between the quadrupolar order and a quantum spin liquid [78]. Such a scenario cannot apply to $Tb_{2+x}Ti_{2-x}O_{7+y}$ since the splitting of the crystal-field levels are weaker in crystal C1 presenting a quadrupolar state, than in C2 with a spin-liquid state, in contradiction with the phase diagram proposed in Ref. [79]. It is also worth noting that in $Tb_2Ti_2O_7$ the first excited doublet should also be taken into account. However, it seems likely that it will not have a significant impact on our interpretation. On one hand, as Eq. (2) shows, the vibronic process will still favor the same orientation of the quadrupoles on a whole tetrahedron. On the second hand, it will probably only slightly modify the phase boundaries and position of $Tb_{2+x}Ti_{2-x}O_{7+y}$ in the phase diagram since the energy of the first excited crystal-field level is about an order of magnitude larger than the energy scale of typical interactions in rare-earth pyrochlores [72]. One more question we can address is the origin of the strong x dependence of vibronic couplings. While a quantitative answer is beyond the scope of this study, the very low value of x for which changes occur suggests that this dependence has a collective origin. One can therefore reasonably think that vibronic processes might be strongly affected by local defects recalling that a vibronic ground state actually results from a hybridization between local degrees of freedom (crystal-field excitations) and collective degrees of freedom (acoustic phonons).

III. CONCLUSION

In summary, using high-resolution synchrotron-based THz spectroscopy coupled with quantum calculations, we show that vibronic processes, namely hybridizations between crystal-field levels and phonons, are strongly affected by a small change of stoichiometry x in $Tb_{2+x}Ti_{2-x}O_{7+y}$. Our measurements reveal that the amplitude of these two processes (one appearing below 200 K and one below 50 K) are greater when $x < 0$ than $x > 0$. All spectra measured in two different samples, at different temperatures, and with magnetic fields (results of Ref. [63]) are qualitatively reproduced by our calculations which use a single, sample-dependent, vibronic coupling parameter. We show that these vibronic couplings affect the ground state in the sense that they promote quadrupolar correlations antagonistic to those resulting from quadrupolar interactions and leading to an order at very low temperature for $x \gtrsim 0$. This quadrupolar order is even destroyed for $x \lesssim 0$ when these vibronic couplings become stronger, and the subtle admixture between magnetic interactions and these two quadrupolar effects in competition leaves a spin-liquid ground state. This scenario is not without similarities with frustrated spin systems where correlations of magnetic dipoles can compete producing unconventional behaviors, in particular the destabilization of the spin ice state

when spin ice and all-in–all-out correlations coexist [5]. In the present case, the very rich behavior of $Tb_{2+x}Ti_{2-x}O_{7+y}$ can be interpreted on the basis of such a frustrating mechanism but based on higher rank multipoles, opening the way to more general cases of multipolar frustration, beyond the case of pyrochlore materials [11,80].

ACKNOWLEDGMENTS

We thank Jérôme Debray for the shaping and orientation of the crystals and Pierre Lachkar for the specific heat measurements. E.C. acknowledges financial support by the Austrian Science Fund (Grant No. P32404-N27).

[1] *Introduction to Frustrated Magnetism: Materials, Experiments, Theory*, edited by C. Lacroix, P. Mendels, and F. Mila (Springer, Berlin, 2011).

[2] A. Kitaev, Anyons in an exactly solved model and beyond, Ann. Phys. **321**, 2 (2006).

[3] M. J. Harris, S. T. Bramwell, D. F. McMorrow, T. Zeiske, and K. W. Godfrey, Geometrical Frustration in the Ferromagnetic Pyrochlore $Ho_2Ti_2O_7$, Phys. Rev. Lett. **79**, 2554 (1997).

[4] J. S. Gardner, M. J. P. Gingras, and J. E. Greedan, Magnetic pyrochlore oxides, Rev. Mod. Phys. **82**, 53 (2010).

[5] M. E. Brooks-Bartlett, S. T. Banks, L. D. C. Jaubert, A. Harman-Clarke, and P. C. W. Holdsworth, Magnetic-Moment Fragmentation and Monopole Crystallization, Phys. Rev. X **4**, 011007 (2014).

[6] E. Lefrançois, V. Cathelin, E. Lhotel, J. Robert, P. Lejay, C. V. Colin, B. Canals, F. Damay, J. Ollivier, B. Fåk, L. C. Chapon, R. Ballou, and V. Simonet, Fragmentation in spin ice from magnetic charge injection, Nat. Commun. **8**, 209 (2017).

[7] V. Cathelin, E. Lefrançois, J. Robert, P. C. Guruciaga, C. Paulsen, D. Prabhakaran, P. Lejay, F. Damay, J. Ollivier, B. Fåk, L. C. Chapon, R. Ballou, V. Simonet, P. C. W. Holdsworth, and E. Lhotel, Fragmented monopole crystal, dimer entropy, and Coulomb interactions in $Dy_2Ir_2O_7$, Phys. Rev. Res. **2**, 032073(R) (2020).

[8] P. Santini, S. Carretta, G. Amoretti, R. Caciuffo, N. Magnani, and G. H. Lander, Multipolar interactions in f-electron systems: The paradigm of actinide dioxides, Rev. Mod. Phys. **81**, 807 (2009).

[9] P. Morin and D. Schmitt, Quadrupolar interactions and magneto-elastic effects in rare earth intermetallic compounds, in *Handbook of Ferromagnetic Materials* (Elsevier, Amsterdam, 1990), Chap. 1, pp. 1–132.

[10] K. Araki, T. Goto, K. Mitsumoto, Y. Nemoto, M. Akatsu, H. S. Suzuki, H. Tanida, S. Takagi, S. Yasin, S. Zherlitsyn, and J. Wosnitza, Dissipation in non-Kramers doublet of $PrMg_3$, J. Phys. Soc. Jpn. **81**, 023710 (2012).

[11] H. Tsunetsugu, T. Ishitobi, and K. Hattori, Quadrupole orders on the fcc lattice, J. Phys. Soc. Jpn. **90**, 043701 (2021).

[12] S. Onoda and Y. Tanaka, Quantum Melting of Spin Ice: Emergent Cooperative Quadrupole and Chirality, Phys. Rev. Lett. **105**, 047201 (2010).

[13] S. Onoda and Y. Tanaka, Quantum fluctuations in the effective pseudospin-1/2 model for magnetic pyrochlore oxides, Phys. Rev. B **83**, 094411 (2011).

[14] Y.-P. Huang, G. Chen, and M. Hermele, Quantum Spin Ices and Topological Phases from Dipolar-Octupolar Doublets on the Pyrochlore Lattice, Phys. Rev. Lett. **112**, 167203 (2014).

[15] S. Petit, E. Lhotel, S. Guitteny, O. Florea, J. Robert, P. Bonville, I. Mirebeau, J. Ollivier, H. Mutka, E. Ressouche, C. Decorse, M. Ciomaga Hatnean, and G. Balakrishnan, Antiferroquadrupolar correlations in the quantum spin ice candidate $Pr_2Zr_2O_7$, Phys. Rev. B **94**, 165153 (2016).

[16] O. Benton, Ground-state phase diagram of dipolar-octupolar pyrochlores, Phys. Rev. B **102**, 104408 (2020).

[17] R. Sibille, N. Gauthier, E. Lhotel, V. Porée, V. Pomjakushin, R. A. Ewings, T. G. Perring, J. Ollivier, A. Wildes, C. Ritter, T. C. Hansen, D. A. Keen, G. J. Nilsen, L. Keller, S. Petit, and T. Fennell, A quantum liquid of magnetic octupoles on the pyrochlore lattice, Nat. Phys. **16**, 546 (2020).

[18] J. Xu, O. Benton, A. T. M. N. Islam, T. Guidi, G. Ehlers, and B. Lake, Order Out of a Coulomb Phase and Higgs Transition: Frustrated Transverse Interactions of $Nd_2Zr_2O_7$, Phys. Rev. Lett. **124**, 097203 (2020).

[19] M. Léger, E. Lhotel, M. Ciomaga Hatnean, J. Ollivier, A. R. Wildes, S. Raymond, E. Ressouche, G. Balakrishnan, and S. Petit, Spin Dynamics and Unconventional Coulomb Phase in $Nd_2Zr_2O_7$, Phys. Rev. Lett. **126**, 247201 (2021).

[20] G. Aeppli, A. V. Balatsky, H. M. Rønnow, and N. A. Spaldin, Hidden, entangled and resonating order, Nat. Rev. Mater. **5**, 477 (2020).

[21] S. W. Lovesey, D. D. Khalyavin, and U. Staub, Ferro-type order of magneto-electric quadrupoles as an order-parameter for the pseudo-gap phase of a cuprate superconductor, J. Phys.: Condens. Matter **27**, 292201 (2015).

[22] M. Fechner, M. J. A. Fierz, F. Thöle, U. Staub, and N. A. Spaldin, Quasistatic magnetoelectric multipoles as order parameter for pseudogap phase in cuprate superconductors, Phys. Rev. B **93**, 174419 (2016).

[23] T. Taniguchi, H. Kadowaki, H. Takatsu, B. Fåk, J. Ollivier, T. Yamazaki, T. J. Sato, H. Yoshizawa, Y. Shimura, T. Sakakibara, T. Hong, K. Goto, L. R. Yaraskavitch, and J. B. Kycia, Long-range order and spin-liquid states of polycrystalline $Tb_{2+x}Ti_{2-x}O_{7+y}$, Phys. Rev. B **87**, 060408(R) (2013).

[24] M. Wakita, T. Taniguchi, H. Edamoto, H. Takatsu, and H. Kadowaki, Quantum spin liquid and electric quadrupolar states of single crystal $Tb_{2+x}Ti_{2-x}O_{7+y}$, J. Phys.: Conf. Ser. **683**, 012023 (2016).

[25] J. S. Gardner, S. R. Dunsiger, B. D. Gaulin, M. J. P. Gingras, J. E. Greedan, R. F. Kiefl, M. D. Lumsden, W. A. MacFarlane, N. P. Raju, J. E. Sonier, I. Swainson, and Z. Tun, Cooperative Paramagnetism in the Geometrically Frustrated Pyrochlore Antiferromagnet $Tb_2Ti_2O_7$, Phys. Rev. Lett. **82**, 1012 (1999).

[26] J. S. Gardner, B. D. Gaulin, A. J. Berlinsky, P. Waldron, S. R. Dunsiger, N. P. Raju, and J. E. Greedan, Neutron scattering studies of the cooperative paramagnet pyrochlore $Tb_2Ti_2O_7$, Phys. Rev. B **64**, 224416 (2001).

[27] T. Fennell, M. Kenzelmann, B. Roessli, M. K. Haas, and R. J. Cava, Power-Law Spin Correlations in the Pyrochlore Antiferromagnet $Tb_2Ti_2O_7$, Phys. Rev. Lett. **109**, 017201 (2012).

[28] S. Petit, P. Bonville, J. Robert, C. Decorse, and I. Mirebeau, Spin liquid correlations, anisotropic exchange, and symmetry breaking in $Tb_2Ti_2O_7$, Phys. Rev. B **86**, 174403 (2012).

[29] M. J. P. Gingras, B. C. den Hertog, M. Faucher, J. S. Gardner, S. R. Dunsiger, L. J. Chang, B. D. Gaulin, N. P. Raju, and J. E. Greedan, Thermodynamic and single-ion properties of Tb^{3+} within the collective paramagnetic-spin liquid state of the frustrated pyrochlore antiferromagnet $Tb_2Ti_2O_7$, Phys. Rev. B **62**, 6496 (2000).

[30] I. Mirebeau, P. Bonville, and M. Hennion, Magnetic excitations in $Tb_2Sn_2O_7$ and $Tb_2Ti_2O_7$ as measured by inelastic neutron scattering, Phys. Rev. B **76**, 184436 (2007).

[31] T. T. A. Lummen, I. P. Handayani, M. C. Donker, D. Fausti, G. Dhalenne, P. Berthet, A. Revcolevschi, and P. H. M. van Loosdrecht, Phonon and crystal field excitations in geometrically frustrated rare earth titanates, Phys. Rev. B **77**, 214310 (2008).

[32] A. Bertin, Y. Chapuis, P. Dalmas de Réotier, and A. Yaouanc, Crystal electric field in the $R_2Ti_2O_7$ pyrochlore compounds, J. Phys.: Condens. Matter **24**, 256003 (2012).

[33] J. Zhang, K. Fritsch, Z. Hao, B. V. Bagheri, M. J. P. Gingras, G. E. Granroth, P. Jiramongkolchai, R. J. Cava, and B. D. Gaulin, Neutron spectroscopic study of crystal field excitations in $Tb_2Ti_2O_7$ and $Tb_2Sn_2O_7$, Phys. Rev. B **89**, 134410 (2014).

[34] V. V. Klekovkina and B. Z. Malkin, Crystal field and magnetoelastic interactions in $Tb_2Ti_2O_7$, Opt. Spectrosc. **116**, 849 (2014).

[35] A. J. Princep, H. C. Walker, D. T. Adroja, D. Prabhakaran, and A. T. Boothroyd, Crystal field states of Tb^{3+} in the pyrochlore spin liquid $Tb_2Ti_2O_7$ from neutron spectroscopy, Phys. Rev. B **91**, 224430 (2015).

[36] M. Ruminy, E. Pomjakushina, K. Iida, K. Kamazawa, D. T. Adroja, U. Stuhr, and T. Fennell, Crystal-field parameters of the rare-earth pyrochlores $R_2Ti_2O_7$ (R = Tb, Dy, and Ho), Phys. Rev. B **94**, 024430 (2016).

[37] Y.-J. Kao, M. Enjalran, A. Del Maestro, H. R. Molavian, and M. J. P. Gingras, Understanding paramagnetic spin correlations in the spin-liquid pyrochlore $Tb_2Ti_2O_7$, Phys. Rev. B **68**, 172407 (2003).

[38] M. Enjalran and M. J. P. Gingras, Theory of paramagnetic scattering in highly frustrated magnets with long-range dipole-dipole interactions: The case of the $Tb_2Ti_2O_7$ pyrochlore antiferromagnet, Phys. Rev. B **70**, 174426 (2004).

[39] H. R. Molavian, M. J. P. Gingras, and B. Canals, Dynamically Induced Frustration as a Route to a Quantum Spin Ice State in $Tb_2Ti_2O_7$ via Virtual Crystal Field Excitations and Quantum Many-Body Effects, Phys. Rev. Lett. **98**, 157204 (2007).

[40] S. H. Curnoe, Structural distortion and the spin liquid state in $Tb_2Ti_2O_7$, Phys. Rev. B **78**, 094418 (2008).

[41] H. R. Molavian and M. J. P. Gingras, Proposal for a [111] magnetization plateau in the spin liquid state of $Tb_2Ti_2O_7$, J. Phys.: Condens. Matter **21**, 172201 (2009).

[42] P. Bonville, I. Mirebeau, A. Gukasov, S. Petit, and J. Robert, Tetragonal distortion yielding a two-singlet spin liquid in pyrochlore $Tb_2Ti_2O_7$, Phys. Rev. B **84**, 184409 (2011).

[43] S. H. Curnoe, Effective spin-1/2 exchange model for $Tb_2Ti_2O_7$, Phys. Rev. B **88**, 014429 (2013).

[44] P. Bonville, A. Gukasov, I. Mirebeau, and S. Petit, Towards a model of a dynamical Jahn-Teller coupling at very low temperatures in $Tb_2Ti_2O_7$, Phys. Rev. B **89**, 085115 (2014).

[45] Y. Gritsenko, S. Mombetsu, P. T. Cong, T. Stöter, E. L. Green, C. S. Mejia, J. Wosnitza, M. Ruminy, T. Fennell, A. A. Zvyagin, S. Zherlitsyn, and M. Kenzelmann, Changes in elastic moduli as evidence for quadrupolar ordering in the rare-earth frustrated magnet $Tb_2Ti_2O_7$, Phys. Rev. B **102**, 060403(R) (2020).

[46] H. Kadowaki, H. Takatsu, T. Taniguchi, B. Fåk, and J. Ollivier, Composite spin and quadrupole wave in the ordered phase of $Tb_{2+x}Ti_{2-x}O_{7+y}$, SPIN **05**, 1540003 (2015).

[47] E. Kermarrec, D. D. Maharaj, J. Gaudet, K. Fritsch, D. Pomaranski, J. B. Kycia, Y. Qiu, J. R. D. Copley, M. M. P. Couchman, A. O. R. Morningstar, H. A. Dabkowska, and B. D. Gaulin, Gapped and gapless short-range-ordered magnetic states with $(\frac{1}{2}, \frac{1}{2}, \frac{1}{2})$ wave vectors in the pyrochlore magnet $Tb_{2+x}Ti_{2-x}O_{7+\delta}$, Phys. Rev. B **92**, 245114 (2015).

[48] H. Takatsu, S. Onoda, S. Kittaka, A. Kasahara, Y. Kono, T. Sakakibara, Y. Kato, B. Fåk, J. Ollivier, J. W. Lynn, T. Taniguchi, M. Wakita, and H. Kadowaki, Quadrupole Order in the Frustrated Pyrochlore $Tb_{2+x}Ti_{2-x}O_{7+y}$, Phys. Rev. Lett. **116**, 217201 (2016).

[49] H. Kadowaki, M. Wakita, B. Fåk, J. Ollivier, S. Ohira-Kawamura, K. Nakajima, H. Takatsu, and M. Tamai, Continuum excitation and pseudospin wave in quantum spin-liquid and quadrupole ordered states of $Tb_{2+x}Ti_{2-x}O_{7+y}$, J. Phys. Soc. Jpn. **87**, 064704 (2018).

[50] H. Kadowaki, M. Wakita, B. Fåk, J. Ollivier, S. Ohira-Kawamura, K. Nakajima, and J. W. Lynn, Spin correlations of quantum spin liquid and quadrupole-ordered states of $Tb_{2+x}Ti_{2-x}O_{7+y}$, Phys. Rev. B **99**, 014406 (2019).

[51] H. Kadowaki, M. Wakita, B. Fåk, J. Ollivier, and S. Ohira-Kawamura, Spin and quadrupole correlations by three-spin interaction in the frustrated pyrochlore magnet $Tb_{2+x}Ti_{2-x}O_{7+y}$, Phys. Rev. B **105**, 014439 (2022).

[52] J. P. C. Ruff, B. D. Gaulin, J. P. Castellan, K. C. Rule, J. P. Clancy, J. Rodriguez, and H. A. Dabkowska, Structural Fluctuations in the Spin-Liquid State of $Tb_2Ti_2O_7$, Phys. Rev. Lett. **99**, 237202 (2007).

[53] Y. Nakanishi, T. Kumagai, M. Yoshizawa, K. Matsuhira, S. Takagi, and Z. Hiroi, Elastic properties of the rare-earth dititanates $R_2Ti_2O_7$ (R = Tb, Dy, and Ho), Phys. Rev. B **83**, 184434 (2011).

[54] K. Goto, H. Takatsu, T. Taniguchi, and H. Kadowaki, Absence of anomalous negative lattice-expansion for polycrystalline sample of $Tb_2Ti_2O_7$, J. Phys. Soc. Jpn. **81**, 015001 (2012).

[55] P. D. de Réotier, A. Yaouanc, A. Bertin, C. Marin, S. Vanishri, D. Sheptyakov, A. Cervellino, B. Roessli, and C. Baines, Low temperature crystal structure and local magnetometry for the geometrically frustrated pyrochlore $Tb_2Ti_2O_7$, J. Phys.: Conf. Ser. **551**, 012021 (2014).

[56] M. Ruminy, F. Groitl, T. Keller, and T. Fennell, Neutron Larmor diffraction investigation of the rare-earth pyrochlores $R_2Ti_2O_7$ (R = Tb, Dy, Ho), Phys. Rev. B **94**, 174406 (2016).

[57] S. Guitteny, J. Robert, P. Bonville, J. Ollivier, C. Decorse, P. Steffens, M. Boehm, H. Mutka, I. Mirebeau, and S. Petit, Anisotropic Propagating Excitations and Quadrupolar Effects in $Tb_2Ti_2O_7$, Phys. Rev. Lett. **111**, 087201 (2013).

[58] T. Fennell, M. Kenzelmann, B. Roessli, H. Mutka, J. Ollivier, M. Ruminy, U. Stuhr, O. Zaharko, L. Bovo, A. Cervellino, M. K. Haas, and R. J. Cava, Magnetoelastic Excitations in the Pyrochlore Spin Liquid $Tb_2Ti_2O_7$, Phys. Rev. Lett. **112**, 017203 (2014).

[59] M. Ruminy, L. Bovo, E. Pomjakushina, M. K. Haas, U. Stuhr, A. Cervellino, R. J. Cava, M. Kenzelmann, and T. Fennell, Sample independence of magnetoelastic excitations in the rare-earth pyrochlore $Tb_2Ti_2O_7$, Phys. Rev. B **93**, 144407 (2016).

[60] M. Ruminy, S. Guitteny, J. Robert, L.-P. Regnault, M. Boehm, P. Steffens, H. Mutka, J. Ollivier, U. Stuhr, J. S. White, B. Roessli, L. Bovo, C. Decorse, M. K. Haas, R. J. Cava, I. Mirebeau, M. Kenzelmann, S. Petit, and T. Fennell, Magnetoelastic excitation spectrum in the rare-earth pyrochlore $Tb_2Ti_2O_7$, Phys. Rev. B **99**, 224431 (2019).

[61] A. A. Turrini, M. Ruminy, F. Bourdarot, U. Stuhr, J. S. White, G. Tucker, M. Skoulatos, M. Núñez-Valdez, and T. Fennell, Magnetic-field control of magnetoelastic coupling in the rare-earth pyrochlore $Tb_2Ti_2O_7$, Phys. Rev. B **104**, 224403 (2021).

[62] E. Constable, R. Ballou, J. Robert, C. Decorse, J.-B. Brubach, P. Roy, E. Lhotel, L. Del-Rey, V. Simonet, S. Petit, and S. deBrion, Double vibronic process in the quantum spin ice candidate $Tb_2Ti_2O_7$ revealed by terahertz spectroscopy, Phys. Rev. B **95**, 020415(R) (2017).

[63] K. Amelin, Y. Alexanian, U. Nagel, T. Rõõm, J. Robert, J. Debray, V. Simonet, C. Decorse, Z. Wang, R. Ballou, E. Constable, and S. de Brion, Terahertz magneto-optical investigation of quadrupolar spin-lattice effects in magnetically frustrated $Tb_2Ti_2O_7$, Phys. Rev. B **102**, 134428 (2020).

[64] P. Thalmeier, Theory of the bound state between phonons and a CEF excitation in $CeAl_2$, J. Phys. C **17**, 4153 (1984).

[65] Y. Alexanian, Couplages entre degrés de liberté dans les pyrochlores magnétiques, Ph.D. thesis, Université Grenoble-Alpes, 2021.

[66] See Supplemental Material at http://link.aps.org/supplemental/10.1103/PhysRevB.107.224404 for the THz spectra in other polarizations than those reported in Fig. 2; the details of the crystal-field and vibronic Hamiltonians, their diagonalization and associated wave functions; the THz absorption calculations with a static magnetic field; the comparison with other optical and inelastic neutron measurements; the pseudospin model and associated order parameter; and the calculations of the angular dependence of the charge density depicted in Fig. 1, which includes Refs. [73,74,81–84].

[67] P. Thalmeier and P. Fulde, Bound State between a Crystal-Field Excitation and a Phonon in $CeAl_2$, Phys. Rev. Lett. **49**, 1588 (1982).

[68] X. Zhang, Y. Luo, T. Halloran, J. Gaudet, H. Man, S. M. Koohpayeh, and N. P. Armitage, Low-energy magneto-optics of $Tb_2Ti_2O_7$ in a [111] magnetic field, Phys. Rev. B **103**, L140403 (2021).

[69] S. B. Lee, S. Onoda, and L. Balents, Generic quantum spin ice, Phys. Rev. B **86**, 104412 (2012).

[70] S. H. Curnoe, Exchange interactions in two-state systems: Rare earth pyrochlores, J. Phys.: Condens. Matter **30**, 235803 (2018).

[71] H. Yan, O. Benton, L. Jaubert, and N. Shannon, Theory of multiple-phase competition in pyrochlore magnets with anisotropic exchange with application to $Yb_2Ti_2O_7$, $Er_2Ti_2O_7$, and $Er_2Sn_2O_7$, Phys. Rev. B **95**, 094422 (2017).

[72] J. G. Rau and M. J. Gingras, Frustrated quantum rare-earth pyrochlores, Annu. Rev. Condens. Matter Phys. **10**, 357 (2019).

[73] D. Schmitt, Angular distribution of 4f electrons in the presence of a crystal field, J. Phys. France **47**, 677 (1986).

[74] H. Kusunose, Description of multipole in f-electron systems, J. Phys. Soc. Jpn. **77**, 064710 (2008).

[75] K. Boldyrev, N. Abishev, I. Mumdzi, S. Nikitin, B. Malkin, R. Yusupov, and M. Popova, High-resolution spectroscopic studies of random strains in ferroelastic domains in the $LaAlO_3$:Tm^{3+} single crystal, Opt. Mater.: X **14**, 100155 (2022).

[76] J.-J. Wen, S. M. Koohpayeh, K. A. Ross, B. A. Trump, T. M. McQueen, K. Kimura, S. Nakatsuji, Y. Qiu, D. M. Pajerowski, J. R. D. Copley, and C. L. Broholm, Disordered Route to the Coulomb Quantum Spin Liquid: Random Transverse Fields on Spin Ice in $Pr_2Zr_2O_7$, Phys. Rev. Lett. **118**, 107206 (2017).

[77] N. Martin, P. Bonville, E. Lhotel, S. Guitteny, A. Wildes, C. Decorse, M. Ciomaga Hatnean, G. Balakrishnan, I. Mirebeau, and S. Petit, Disorder and Quantum Spin Ice, Phys. Rev. X **7**, 041028 (2017).

[78] L. Savary and L. Balents, Disorder-Induced Quantum Spin Liquid in Spin Ice Pyrochlores, Phys. Rev. Lett. **118**, 087203 (2017).

[79] O. Benton, Instabilities of a U(1) Quantum Spin Liquid in Disordered Non-Kramers Pyrochlores, Phys. Rev. Lett. **121**, 037203 (2018).

[80] K. Hattori and H. Tsunetsugu, Classical Monte Carlo study for antiferro quadrupole orders in a diamond lattice, J. Phys. Soc. Jpn. **85**, 094001 (2016).

[81] K. W. H. Stevens, Matrix elements and operator equivalents connected with the magnetic properties of rare earth ions, Proc. Phys. Soc., Sect. A **65**, 209 (1952).

[82] M. T. Hutchings, Point-charge calculations of energy levels of magnetic ions in crystalline electric fields, Solid State Phys. **16**, 227 (1964).

[83] O. Danielsen and P.-A. Lindgård, *Quantum Mechanical Operator Equivalents Used in the Theory of Magnetism* (Risø National Laboratory, Roskilde, Denmark, 1972).

[84] K. Momma and F. Izumi, VESTA 3 for three-dimensional visualization of crystal, volumetric and morphology data, J. Appl. Crystallogr. **44**, 1272 (2011).